

# Ionic Liquid Electrolytes with Various Sodium Solutes for Rechargeable Na/NaFePO<sub>4</sub> Batteries Operated at Elevated Temperatures

Nithinai Wongittharom,<sup>†</sup> Chueh-Han Wang,<sup>‡</sup> Yi-Chen Wang,<sup>‡</sup> Cheng-Hsien Yang,<sup>‡</sup> and Jeng-Kuei Chang<sup>\*,†,‡,§</sup>

<sup>†</sup>Department of Chemical and Materials Engineering, National Central University, Jhongli 32001, Taiwan

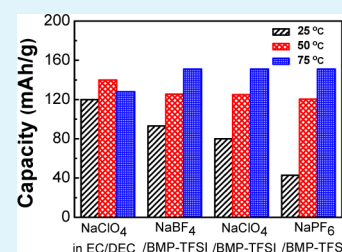
<sup>‡</sup>Institute of Materials Science and Engineering, National Central University, Jhongli 32001, Taiwan

<sup>§</sup>Department of Mechanical Engineering, National Central University, Jhongli 32001, Taiwan

## S Supporting Information

**ABSTRACT:** NaFePO<sub>4</sub> with an olivine structure is synthesized via chemical delithiation of LiFePO<sub>4</sub> followed by electrochemical sodiation of FePO<sub>4</sub>. Butylmethylpyrrolidinium-bis(trifluoromethanesulfonyl)imide (BMP-TFSI) ionic liquid (IL) with various sodium solutes, namely NaBF<sub>4</sub>, NaClO<sub>4</sub>, NaPF<sub>6</sub>, and NaN(CN)<sub>2</sub>, is used as an electrolyte for rechargeable Na/NaFePO<sub>4</sub> cells. The IL electrolytes show high thermal stability (>350 °C) and nonflammability, and are thus ideal for high-safety applications. The highest conductivity and the lowest viscosity of the electrolyte are obtained with NaBF<sub>4</sub>. At an elevated temperature (above 50 °C), the IL electrolyte is more suitable than a conventional organic electrolyte for the sodium cell. At 75 °C, the measured capacity of NaFePO<sub>4</sub> in a NaBF<sub>4</sub>-incorporated IL electrolyte is as high as 152 mAh g<sup>-1</sup> (at 0.05 C), which is near the theoretical value (154 mAh g<sup>-1</sup>). Moreover, 60% of this capacity can be retained when the charge–discharge rate is increased to 1 C.

**KEYWORDS:** sodium-ion battery, NaFePO<sub>4</sub>, ionic liquid electrolyte, Na solute, temperature



## INTRODUCTION

Lithium (Li)-ion batteries (LIBs) are the dominant charge-storage units for consumer portable electronic devices due to their high energy and power densities.<sup>1–3</sup> However, the implementation of a Li-based technology for mass energy storage (e.g., for automotive transportation and grid-related applications) faces an important challenge associated with both Li availability and cost.<sup>4–6</sup> Using a sodium (Na)-based technology as an alternative is attractive because Na is more abundant than Li and is easy to recycle.<sup>7</sup> Na and Li possess analogous physicochemical properties (and thus the known LIB knowledge can be exploited), making sodium-ion batteries (SIBs) a recent research interest.<sup>8,9</sup> Nevertheless, the performance of SIBs is not satisfactory to date because Na-based chemistry has been studied much less than has Li-based chemistry.<sup>10,11</sup> With further investigations, great improvement in SIB performance is expected.

The electrolyte is a key component that governs the electrochemistry in a battery.<sup>7,12</sup> Although a number of efforts are being directed toward the search for new electrode materials for SIBs, electrolytes have received less attention. In our opinion, more development of the electrolyte is necessary before SIBs can become practical. Aqueous and organic electrolytes have been applied to SIBs.<sup>6,13</sup> Owing to larger potential stability windows, organic-electrolyte cells have higher energy and power densities (as compared to aqueous-electrolyte cells). Ponrouch et al. indicated that the types of

organic solvent and Na solute are important factors that affect the electrochemical properties of SIBs.<sup>14</sup> However, organic electrolytes typically have low heat capacity, poor thermal stability, and high volatility and flammability, making them a safety risk, especially for large-scale energy storage.<sup>15–17</sup> Ionic liquids (ILs), characterized by excellent thermal stability, nonvolatility, large electrochemical windows, and intrinsic ionic conductivity,<sup>18–20</sup> are a promising alternative electrolyte for SIBs. Hagiwara et al. proposed inorganic NaFSI/KFSI (FSI = bis(fluorosulfonyl)imide) intermediate-temperature IL electrolytes (with melting points of ~65 °C depending on the NaFSI/KFSI ratio) for NaCrO<sub>2</sub>, Na<sub>2</sub>FeP<sub>2</sub>O<sub>7</sub>, and Sn electrodes; this electrolyte has been demonstrated to have considerable potential for use in SIBs.<sup>21–23</sup> Recently, effects of added NaTFSI (FSI = bis(trifluoromethylsulfonyl)imide) concentration on the density, viscosity, conductivity, thermal stability, and solvation property of imidazolium-TFSI and pyrrolidinium-TFSI ILs at various temperatures have been investigated.<sup>24–26</sup> It was concluded that these IL electrolytes are promising for SIBs. However, how they work in a full cell (i.e., with cathodes) requires further study. Actually, research on IL electrolytes is rather limited. For example, the effects of the Na solute type in ILs, crucial for SIB performance, have never been

Received: May 28, 2014

Accepted: September 22, 2014

Published: October 8, 2014

explored. This issue is thus the main subject of the present study.

For SIBs, the high-rate charge-storage performance is usually not satisfactory at room temperature. This is attributed to the larger size of  $\text{Na}^+$  ions (than  $\text{Li}^+$  ions), which is unfavorable for transport in electrodes.<sup>27,28</sup> Slightly heating the cell can improve the charge–discharge kinetics and is practicable in electric vehicle and stationary storage applications. Nevertheless, a previous report indicated that cyclic stability of organic-electrolyte SIBs considerably decayed at 60 °C.<sup>29</sup> Using IL electrolytes, which have high thermal stability, may enable superior SIB performance at elevated temperatures. The effect of temperature on the charge–discharge behavior of an IL-electrolyte SIB is systematically studied herein.

In this work, a promising SIB cathode,  $\text{NaFePO}_4$ , with great thermal stability and large theoretical capacity ( $154 \text{ mAh g}^{-1}$ )<sup>30</sup> is studied in room-temperature butylmethylpyrrolidinium-bis(trifluoromethylsulfonfyl)imide (BMP–TFSI)-based ILs. This cation/anion combination is used because its cathodic limit (associated with the decomposition of  $\text{BMP}^+$ ) is beyond the Na redox potential and the TFSI<sup>−</sup> can withstand a highly oxidative condition ( $>5.0 \text{ V vs Na}$ );<sup>31</sup> the feasibility of this type of IL for SIBs was confirmed.<sup>32</sup> Four types of Na solutes, namely sodium tetrafluoroborate ( $\text{NaBF}_4$ ), sodium perchlorate ( $\text{NaClO}_4$ ), sodium hexafluorophosphate ( $\text{NaPF}_6$ ), and sodium dicyanamide ( $\text{NaN}(\text{CN})_2$ ), are dissolved in the IL to endow it with  $\text{Na}^+$  transport ability. The charge–discharge properties of the Na/ $\text{NaFePO}_4$  cells with these IL electrolytes are evaluated at various temperatures (25–75 °C).

## EXPERIMENTAL SECTION

**Sample Preparation.** A carbothermal reduction method was used to synthesize carbon-coated  $\text{LiFePO}_4$  powder at 700 °C. The detailed procedures can be found in the literature.<sup>33</sup>  $\text{FePO}_4$  was then prepared by delithiation of the obtained carbon-coated  $\text{LiFePO}_4$  according to our previous paper.<sup>32</sup> BMP–TFSI IL was prepared and purified (from BMP-Cl (98 wt %, Solvionic) and LiTFSI (99 wt %, Solvionic) precursors) following a published method.<sup>34</sup> The IL was washed with dichloromethane (99 wt %, Showa), filtrated to remove precipitates, and then vacuum-dried at 100 °C for 12 h before use. Four kinds of Na solutes, namely  $\text{NaBF}_4$  (99 wt %, Acros),  $\text{NaClO}_4$  (99 wt %, Acros),  $\text{NaPF}_6$  (99 wt %, Acros), and  $\text{NaN}(\text{CN})_2$  (99 wt %, Acros), each with a concentration of 1 M, were respectively dissolved in BMP–TFSI IL to provide  $\text{Na}^+$  conduction. Each mixture was continuously stirred by a magnetic paddle for 24 h to ensure uniformity. The electrolyte water contents, measured using a Karl Fisher titrator, were in a range of 80–100 ppm. An ethylene carbonate (EC, 99 wt %, Alfa Aesar)/diethyl carbonate (DEC, 99 wt %, Alfa Aesar) conventional organic solvent (1:1 by volume) with 1 M  $\text{NaClO}_4$  solute was also prepared for comparison. The IL and organic electrolytes were handled and stored in an argon-filled glovebox (Innovation Technology Co. Ltd.), where both the moisture content and oxygen content were maintained below 1 ppm.

**Cell Assembly.** A cathode slurry was prepared by mixing 75 wt % synthesized  $\text{FePO}_4$  powder, 20 wt % carbon black, and 5 wt % poly(vinylidene fluoride) in *N*-methyl-2-pyrrolidone solution. The slurry was pasted onto Al foil and vacuum-dried at 110 °C for 2 h (the dried layer was  $\sim 40 \mu\text{m}$  in thickness). After being roll-pressed, the cathode electrode was punched to match the required dimensions (1.3 cm in diameter) of a CR2032 coin cell. The loading amount and the final thickness of the coating layer were approximately 2.5 mg and 25  $\mu\text{m}$ , respectively. Na foil and a polypropylene membrane (Celgard 3501) were used as the anode and the separator, respectively. The assembly of the coin cell was performed in the argon-filled glovebox. According to the literature,<sup>35</sup> sodiation of the  $\text{FePO}_4$  electrode (to

form  $\text{NaFePO}_4$ ) can be performed in the first discharge process of the assembled cell.

**Characterization.** The microstructure of the synthesized  $\text{FePO}_4$  was examined with scanning electron microscopy (SEM; FEI Inspect F50) and transmission electron microscopy (TEM; JEOL 2100F). X-ray diffraction (XRD; Bruker D8 ADVANCE) was employed to study the crystallinity. The thermal stability of the electrolytes was evaluated by a thermogravimetric analysis (TGA; PerkinElmer TGA7). Under a nitrogen atmosphere, the electrolyte samples were heated at a rate of 5 °C  $\text{min}^{-1}$ . To test the electrolyte flammability under air, an established procedure was used.<sup>36</sup> The electrolyte conductivity was measured in the argon-filled glovebox to avoid water and oxygen interference (a TetraCon 325 conductivity meter was used). A dc polarization and impedance spectroscopy combined method, as proposed by Bruce et al.,<sup>37</sup> was adopted to estimate the  $\text{Na}^+$  transference number ( $T_{\text{Na}^+}$ ) in the IL electrolyte. This method was also used to evaluate  $T_{\text{Li}^+}$  in ILs.<sup>38</sup> It is noted that  $\text{Na}^+$  ions can form contact ion pairs and aggregates in the electrolytes; therefore, the measured  $T_{\text{Na}^+}$  data are apparent values. The capacity, high-rate capability, and cyclic stability of the Na/ $\text{NaFePO}_4$  cells with various electrolytes was evaluated at various temperatures (in a voltage range of 2.0–3.8 V) using an Arbin BT-2043 tester. Electrochemical impedance spectroscopic (EIS) analyses were conducted at a cell voltage of 3.0 V and at a full desodiation state to characterize to interface properties at the electrodes. The frequency range and the AC amplitude for the EIS study were  $10^5$ – $10^{-1}$  Hz and 10 mV, respectively.

## RESULTS AND DISCUSSION

The typical morphology of the synthesized  $\text{FePO}_4$  powder, examined using SEM, is shown in Figure 1a. The phosphate

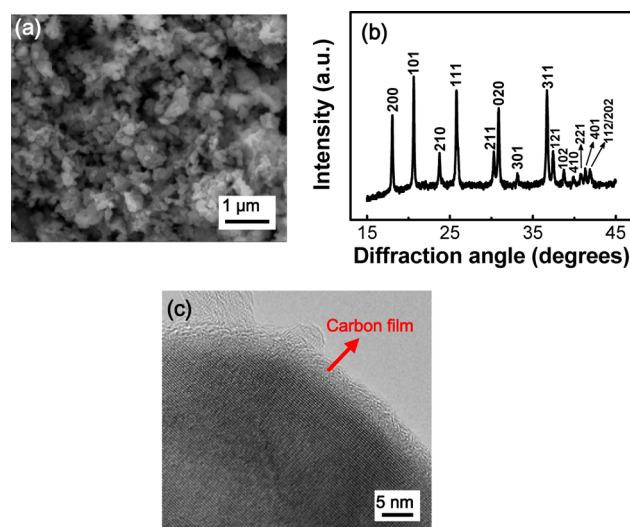


**Figure 1.** (a) SEM micrograph, (b) XRD pattern, and (c) TEM image of synthesized  $\text{FePO}_4$  powder.

particles are uniform and approximately 100 nm in diameter; the small size shortens the  $\text{Na}^+$  diffusion pathway and thus is beneficial for electrode charge–discharge performance. The XRD pattern of the  $\text{FePO}_4$  powder is shown in Figure 1b, which indicates that a single olivine phase with an orthorhombic structure (JCPDS card no. 42-0579) was obtained. This structure, preserved from the original  $\text{LiFePO}_4$  (before delithiation), is favorable for  $\text{Na}^+$  insertion/desertion.<sup>39</sup> Figure 1c shows a high-resolution TEM image of an  $\text{FePO}_4$  particle. There is a carbon film (confirmed via an energy-dispersive spectrometer) on the  $\text{FePO}_4$  crystal. This coating layer, converted from polyethylene glycol (PEG), provides electronic conduction between particles, improving the

electrode charge–discharge properties.<sup>33</sup> Because this layer is  $\text{Li}^+$ -penetrable, it adheres well to the powder surface even after the delithiation process.

Figure 2 shows the TGA data of the conventional organic electrolyte and various IL electrolytes. As shown, the organic

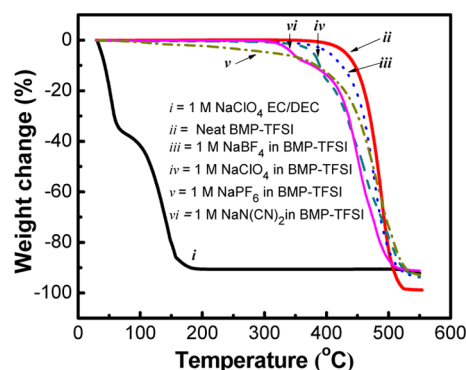


**Figure 2.** TGA data of conventional organic electrolyte (1 M  $\text{NaClO}_4$  in EC/DEC (1/1, v/v) solvent) and BMP–TFSI ILs without and with various Na solutes. The measurements were performed at a heating rate of  $5\text{ }^\circ\text{C min}^{-1}$  under a nitrogen atmosphere.

electrolyte exhibited a significant weight loss of  $>40\%$  before the temperature reached  $100\text{ }^\circ\text{C}$ , at which point the carbonate solvent vigorously evaporated.<sup>40</sup> In contrast, the neat BMP–TFSI IL showed a much higher thermal stability ( $\sim 400\text{ }^\circ\text{C}$ ). It was found that incorporation of  $\text{NaBF}_4$ ,  $\text{NaClO}_4$ , and  $\text{NaN}(\text{CN})_2$  solutes slightly decreased the decomposition temperature to  $330\text{--}360\text{ }^\circ\text{C}$ . For the IL with  $\text{NaPF}_6$ , a gradual weight loss was observed above  $\sim 100\text{ }^\circ\text{C}$ , suggesting that  $\text{NaPF}_6$  is relatively unstable among the Na solutes. It was found that the residual weights of the electrolytes after tests (up to  $550\text{ }^\circ\text{C}$ ) were  $\sim 8\text{ wt } \%$ . This is associated with the fact that the decomposition products of the Na salts remained in the TGA crucibles. Although the TGA is a dynamic test, which overestimates the thermal limit of the electrolytes, the above results clearly reveal that the ILs are more suitable than the conventional organic electrolyte for use at high temperature.

The flammability of various electrolytes is exhibited in Figure S1 (Supporting Information). As shown, the organic electrolyte violently ignited. The self-extinguishing time (after the burner was removed) was approximately  $\sim 50\text{ s g}^{-1}$  (average of 10 samples). In contrast, for the IL electrolytes (regardless of the incorporated Na solutes), there was no ignition observed. The results suggest that this type of electrolyte is promising for high-safety applications.

The ionic conductivity of the IL electrolytes with various Na solutes was acquired as a function of temperature; the data are shown in Figure 3. At  $25\text{ }^\circ\text{C}$ , the measured ionic conductivity of neat BMP–TFSI IL was  $2.2\text{ mS cm}^{-1}$ , which is consistent with a previously reported value.<sup>41</sup> With incorporation of Na solutes, the electrolyte conductivity decreased. This is attributed to the increased electrolyte viscosity (see Figure S2 in the Supporting Information), which results from the interaction between  $\text{Na}^+$  and anions, forming large ion pairs and/or ion clusters.<sup>24–26</sup> The ILs with 1 M  $\text{NaBF}_4$ ,  $\text{NaN}(\text{CN})_2$ ,  $\text{NaClO}_4$ , and  $\text{NaPF}_6$  showed conductivity values of 1.9, 1.5, 1.0, and  $0.5\text{ mS cm}^{-1}$ , respectively. The ion speciations in various ILs need further analyses. Also shown in Figure 3 is IL conductivity increasing (regardless of the Na solute type) with increasing temperature. For example, the ionic conductivity of the 1 M  $\text{NaBF}_4$ /BMP–

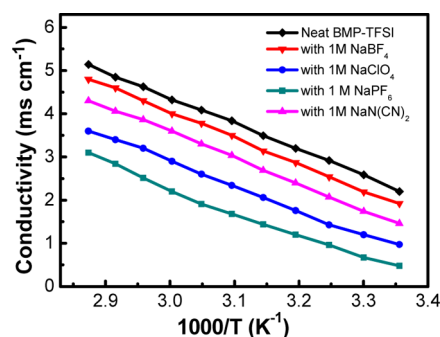


**Figure 3.** Temperature-dependent ionic conductivity of BMP–TFSI ILs without and with various Na solutes.

TFSI IL monotonically increased up to  $4.8\text{ mS cm}^{-1}$  at  $75\text{ }^\circ\text{C}$ . An increase in temperature decreased the electrolyte viscosity (Figure S2, Supporting Information) and promoted the dissociation of the ion pairs or ion clusters,<sup>42</sup> improving the ion mobility in the ILs.

Curve i in Figure 4a shows the  $25\text{ }^\circ\text{C}$  charge–discharge voltage profiles of the  $\text{NaFePO}_4$  electrode (vs Na) recorded in the conventional organic electrolyte at  $0.05\text{ C}$  ( $1\text{ C} = 154\text{ mAh g}^{-1}$ ). As exhibited, the  $\text{Na}/\text{NaFePO}_4$  cell voltage was approximately  $3\text{ V}$ ; the discharge capacity of  $\text{NaFePO}_4$  was  $120\text{ mAh g}^{-1}$  (calculated based on the weight of fully sodiated  $\text{NaFePO}_4$ ), which is close to the theoretical value of  $154\text{ mAh g}^{-1}$ .<sup>30</sup> Moreover, a satisfactory  $\text{NaFePO}_4$  capacity of  $60\text{ mAh g}^{-1}$  was obtained when the charge–discharge rate was increased to  $1\text{ C}$  (see Figure S3, Supporting Information). These values are comparable to or even better than the best values (i.e.,  $120\text{ mAh g}^{-1}@0.05\text{ C}$ ;  $40\text{ mAh g}^{-1}@1\text{ C}$ ) reported for an organic electrolyte,<sup>30</sup> indicating that the prepared cathode is of high quality. It is noted that there were two potential plateaus in the charging curve. This is associated with the formation of an intermediate  $\text{Na}_{0.7}\text{FePO}_4$  phase during the phase transition from  $\text{NaFePO}_4$  to  $\text{FePO}_4$ .<sup>43</sup>

The charge–discharge profiles of the  $\text{Na}/\text{NaFePO}_4$  cells with various IL electrolytes measured at  $25\text{ }^\circ\text{C}$  are also shown in Figure 4a. The discharge (sodiation) capacities found in the  $\text{NaBF}_4$ ,  $\text{NaClO}_4$ , and  $\text{NaPF}_6$ -incorporated IL electrolytes were 92, 79, and  $44\text{ mAh g}^{-1}$ , respectively. The  $\text{NaN}(\text{CN})_2$ -incorporated IL electrolyte was also used. However, the cell charge–discharge voltage was not stable (there were many spikes in the profiles; see Figure S4, Supporting Information). This phenomenon is related to the fact that this electrolyte separated into two phases (an upper clear layer and a lower muddy layer) after a few hours of storage. Figure S4 (Supporting Information) also indicates that the charge capacity was much larger than the discharge counterpart. The origin of this irreversible anodic reaction is not clear so far. However, it is evident that  $\text{NaN}(\text{CN})_2$  is not suitable for use in the BMP–TFSI IL electrolyte.

Figure 4b compares the rate capability of the cells with various electrolytes at  $25\text{ }^\circ\text{C}$ . As shown, the capacity retained ratios at  $0.5\text{ C}$  (compared to those at  $0.05\text{ C}$ ) are 51, 26, and  $17\%$ , respectively, in the  $\text{NaBF}_4$ ,  $\text{NaClO}_4$ , and  $\text{NaPF}_6$ -incorporated IL electrolytes. This coincides with the conductivity and viscosity trend shown in Figures 3 and S2 (Supporting Information). As shown in Figure 4a,b, the performance of the IL-electrolyte cells is inferior to that of a conventional organic-electrolyte cell. It is found that the  $T_{\text{Na}^+}$  values of the three kinds of IL are close ( $0.18\text{--}0.20$ ) but are



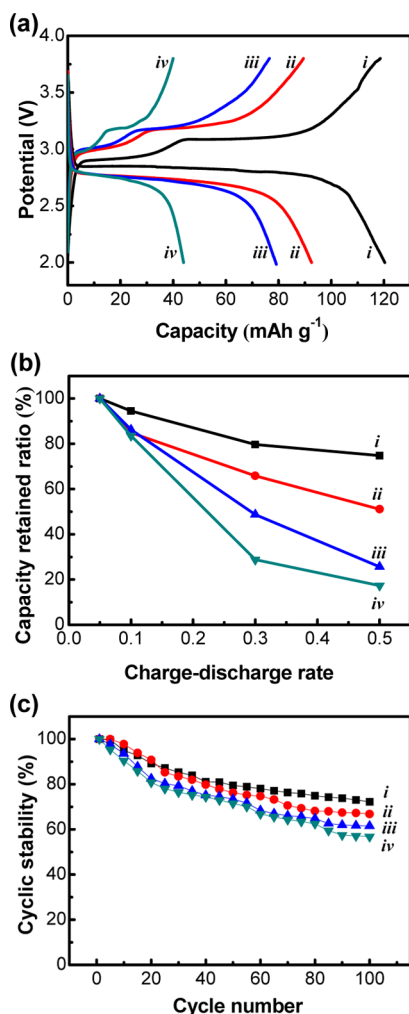
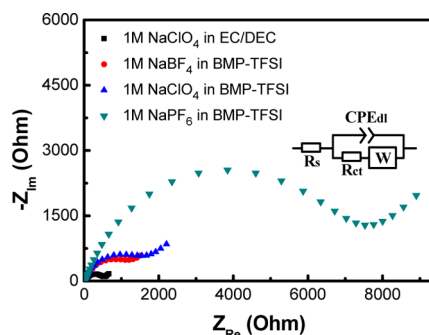


**Figure 4.** (a) Charge–discharge curves at 0.05 C, (b) capacity retained ratios at various charge–discharge rates compared to that obtained at 0.05 C, and (c) cyclic stability of Na/NaFePO<sub>4</sub> cells (measured at 0.3 C) with 1 M NaClO<sub>4</sub> in EC/DEC electrolyte (curve i) and BMP–TFSI IL electrolytes with 1 M NaBF<sub>4</sub> (curve ii), NaClO<sub>4</sub> (curve iii), and NaPF<sub>6</sub> (curve iv). Data are recorded at 25 °C.

considerably lower than that (0.6) for the organic electrolyte (with an ionic conductivity of  $\sim 6.3$  mS cm<sup>-1</sup>), leading to poorer performance of the IL cells.

Electrochemical impedance spectroscopy (EIS) analyses were conducted to study the interface properties at the electrodes. Figure 5 shows the obtained Nyquist plots of the cells with the organic and IL electrolytes. The acquired EIS spectra can be characterized by the inset equivalent circuit in the figure, where the  $R_s$ ,  $R_{ct}$ , CPE<sub>dl</sub>, and  $W$  are electrolyte resistance, charge transfer resistance, Warburg impedance, and the constant phase element related to surface double layer, respectively.<sup>44</sup> It is found that  $R_{ct}$  is distinctly larger than  $R_s$  in each case, indicating that the former is the rate limiting factor for the charge–discharge reaction. The fitting results of  $R_{ct}$  in the organic electrolyte and the NaBF<sub>4</sub>, NaClO<sub>4</sub>, NaTFSI, and NaPF<sub>6</sub>-incorporated IL electrolytes are 480, 1220, 1620, and 7240  $\Omega$ , respectively. Among the IL-electrolyte cells, the optimal properties of the NaBF<sub>4</sub> solute can thus be mainly attributed to the lowest interface resistance at the electrode.

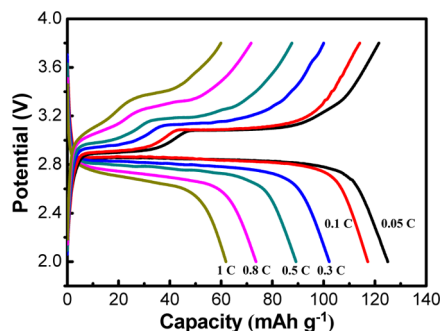
Figure 4c shows the cyclic stability of various cells at 25 °C. After 100 cycles, the organic-electrolyte cell retained 72% of its



**Figure 5.** Nyquist plots of Na/NaFePO<sub>4</sub> cells with organic electrolyte and BMP–TFSI IL electrolytes containing various Na solutes measured at 25 °C.

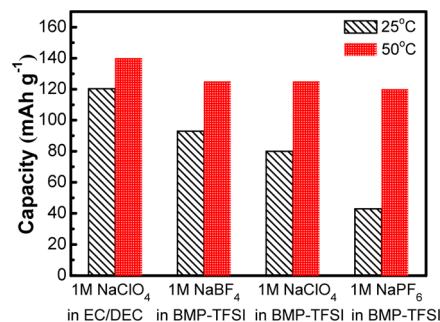
initial capacity. For the IL electrolytes with 1 M NaBF<sub>4</sub>, NaClO<sub>4</sub>, and NaPF<sub>6</sub>, 67%, 62%, and 57% capacities were respectively preserved after the same number of charge–discharge cycles. The capacity decay is ascribed to the active material dissolution and the undesired interaction between the electrode and electrolyte, deteriorating the cell performance upon cycling. The detailed mechanism responsible for the inferior stability in certain IL electrolytes needs further confirmation.

Figure 6 shows the charge–discharge curves of the Na/NaFePO<sub>4</sub> cell with a 1 M NaBF<sub>4</sub>-incorporated IL electrolyte



**Figure 6.** Charge–discharge voltage profiles of Na/NaFePO<sub>4</sub> cell with 1 M NaBF<sub>4</sub>-incorporated BMP–TFSI IL recorded at various charge–discharge rates at 50 °C.

recorded at 50 °C. It was found that slightly increasing the temperature from 25 °C (see Figure 4) to 50 °C caused a significant improvement in the cell capacity and high-rate capability. Figure 7 summarizes the NaFePO<sub>4</sub> discharge capacities



**Figure 7.** Comparison of NaFePO<sub>4</sub> discharge capacities (at 0.05 C) in various electrolytes at 25 and 50 °C.

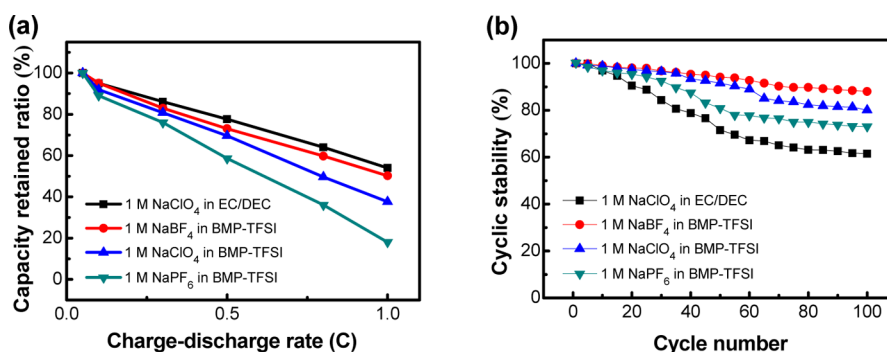


**Figure 8.** (a) Capacity retained ratios at various charge–discharge rates (compared to 0.05 C) and (b) cyclic stability (measured at 0.3 C) of Na/NaFePO<sub>4</sub> cells with various kinds of electrolytes at 50 °C.

(at 0.05 C) in various electrolytes at 25 and 50 °C. Although the capacity found in the organic electrolyte slightly improved from 120 mAh g<sup>-1</sup> (at 25 °C) to 140 mAh g<sup>-1</sup> (at 50 °C), the temperature rise led to considerable capacity increases of NaFePO<sub>4</sub> in the IL electrolytes. At 50 °C, with the NaBF<sub>4</sub>, NaClO<sub>4</sub>, and NaPF<sub>6</sub>-incorporated IL electrolytes, the discharge capacities were 125, 125, and 120 mAh g<sup>-1</sup>, respectively. At such temperatures, the effects of the Na solute type on the low-C-rate capacity are less pronounced than those at 25 °C.

Figure 8a shows the rate capability of the cells at 50 °C. Regardless of the electrolyte type, the capacity retained ratios at high charge–discharge rates clearly increased compared to those found at 25 °C (Figure 4b). This is mainly associated with the reduction of  $R_{ct}$  at the elevated temperature (as summarized in Table 1). As shown, the cell with 1 M NaBF<sub>4</sub>-

**Table 1. Charge Transfer Resistance ( $R_{ct}$ ,  $\Omega$ ), Obtained from EIS Analyses, of Na/NaFePO<sub>4</sub> Cells with Various Electrolytes Measured at 25, 50, and 75 °C**

	organic electrolyte	IL with NaBF <sub>4</sub>	IL with NaClO <sub>4</sub>	IL with NaPF <sub>6</sub>
25 °C	480	1220	1620	7240
50 °C	252	490	917	4680
75 °C	104	174	226	2260

incorporated IL show satisfactory high-rate performance; at 1 C, about 50% of the capacity (at 0.05 C) can be retained, which is comparable to that (54%) for the organic-electrolyte cell. Figure 8b indicates that the capacity retentions after 100 charge–discharge cycles for the cells with IL electrolytes with 1 M NaBF<sub>4</sub>, NaClO<sub>4</sub>, and NaPF<sub>6</sub> are 88%, 80%, and 73%, respectively, at 50 °C. These ratios are much higher than that (62%) for the organic-electrolyte cell. At 50 °C, which is usually encountered in practical applications, employing an IL electrolyte is beneficial for cell cyclic stability. Of note, the type of Na solute affects the performance of the IL electrolyte.

Figure 9 summarizes the effects of temperature (25, 50, and 75 °C) on the performance of the Na/NaFePO<sub>4</sub> cells with the conventional organic electrolyte and the 1 M NaBF<sub>4</sub>-incorporated IL electrolyte. As shown in Figure 9a,b, while the maximum capacity and high-rate performance in the organic electrolyte decrease above 50 °C, those for the IL electrolyte continuously increase with temperature and become superior to those found for the former electrolyte at 75 °C. The measured discharge capacity of NaFePO<sub>4</sub> in the IL electrolyte was as high as 152 mAh g<sup>-1</sup> (at 0.05 C) at 75 °C; 60% of this capacity can be retained when the charge–discharge rate is

increased to 1 C (the charge–discharge curves are shown in Figure S5, Supporting Information). At high temperatures, the organic electrolyte is volatile and unstable (according to the TGA data); in contrast, the IL (with a decomposition temperature of higher than 350 °C) becomes less viscous and thus has increased ionic conductivity ( $T_{Na^+}$  also increases to  $\sim 0.3$  at 75 °C). As a result, the use of an IL electrolyte is favorable for operation temperatures above 50 °C.

The charge–discharge stability of the cells with two kinds of electrolyte as a function of temperature is shown in Figure 9c. The capacity fading rate after 100 cycles in the organic electrolyte clearly accelerated from 28% to 70% when the temperature was increased from 25 to 75 °C. Recently, fluorinated ethylene carbonate was found to be an efficient additive to improve electrode reversibility;<sup>45</sup> its influence on the high-temperature stability of SIBs needs further investigation. In contrast, the cell with the IL electrolyte showed improved cyclability at high temperature (only 10% capacity decay was found at 75 °C after the same number of cycles). The nonvolatility (thus no evaporation problem) and chemical benignity (thus low attack on electrodes) of the IL contribute to the great cell durability at high temperature. According to the data in Figure 9, only for the IL electrolyte does increasing temperature improve the SIB performance in terms of maximum capacity, high-rate capability, and cyclic life. Of note, the IL electrolyte is also more stable and safer (according to Figures 2 and 3) than the conventional organic electrolyte.

## CONCLUSIONS

BMP–TFSI-based ILs, which have a high decomposition temperature (can be >350 °C depending on the Na solute) and nonflammability, are promising electrolytes for use in high-safety SIBs. Among the Na solutes studied, NaBF<sub>4</sub> is the most suitable in the IL (because the highest ionic conductivity and the lowest  $R_{ct}$  can be obtained) to optimize the Na/NaFePO<sub>4</sub> cell performance. In the NaBF<sub>4</sub>-incorporated IL electrolyte, the capacity, high-rate capability, and cyclic life of the Na/NaFePO<sub>4</sub> cell significantly improved with increasing temperature. At 75 °C, an optimal NaFePO<sub>4</sub> capacity of 152 mAh g<sup>-1</sup> (at 0.05 C) was obtained; about 60% of this capacity can be retained when the charge–discharge rate increased to 1 C. After 100 charge–discharge cycles, the capacity decay was only 10%. These properties clearly better than those measured for a conventional organic electrolyte at the elevated temperature, which is encountered in certain applications, such as electric vehicles and stationary energy storage. The proposed IL electrolyte thus has great potential for use in SIBs.

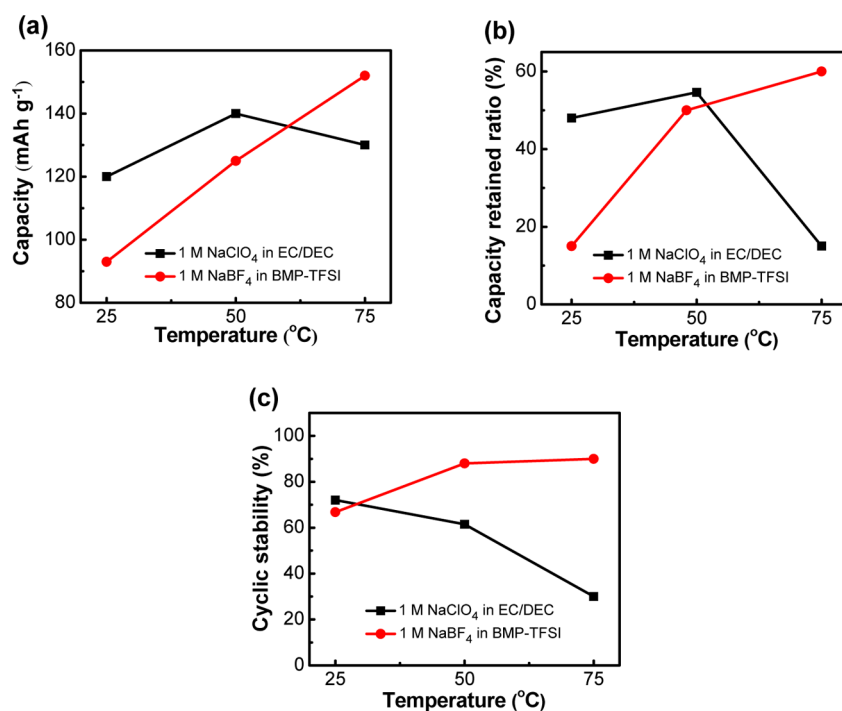


**Figure 9.** Effects of temperature on (a) discharge capacity at 0.05 C, (b) capacity retained ratios at 1 C (compared to that at 0.05 C), and (c) cyclic stability of Na/NaFePO<sub>4</sub> cells incorporating conventional organic electrolyte and IL electrolyte with 1 M NaBF<sub>4</sub>.

## ■ ASSOCIATED CONTENT

### Supporting Information

Flammability tests of organic and IL electrolytes. Viscosity of the IL electrolytes at various temperatures. Charge–discharge voltage profiles of Na/NaFePO<sub>4</sub> cells with conventional organic electrolyte (at 25 °C), with 1 M NaN(CN)<sub>2</sub>-incorporated BMP–TFSI IL electrolyte (at 25 °C), and with 1 M NaBF<sub>4</sub>-incorporated BMP–TFSI IL electrolyte (at 75 °C). This material is available free of charge via the Internet at <http://pubs.acs.org>.

## ■ AUTHOR INFORMATION

### Corresponding Author

\*J.-K. Chang. E-mail: [jkchang@ncu.edu.tw](mailto:jkchang@ncu.edu.tw). Fax: +886-3-2805034. Tel: +886-3-4227151 ext. 34908.

### Notes

The authors declare no competing financial interest.

## ■ ACKNOWLEDGMENTS

The financial support of this work by Ministry of Science and Technology of Taiwan is gratefully appreciated.

## ■ REFERENCES

- (1) Yoshio, M.; Brodd, R. J.; Kozawa, A. In *Lithium-Ion Batteries: Science and Technologies*; Brodd, R. J., Ed.; Springer: New York, 2010; Chapter 1, pp 1–7.
- (2) Liu, J.; Zhang, J. G.; Yang, Z.; Lemmon, J. P.; Imhoff, C.; Graff, G. L.; Li, L.; Hu, J.; Wang, C.; Xiao, J.; Xia, G.; Viswanathan, V. V.; Baskaran, S.; Sprenkle, V.; Li, X.; Shao, Y.; Schwenzler, B. Materials Science and Materials Chemistry for Large Scale Electrochemical Energy Storage: From Transportation to Electrical Grid. *Adv. Funct. Mater.* **2013**, *23*, 929–946.
- (3) Yang, Z.; Zhang, J.; Kintner-Meyer, M. C. W.; Lu, X.; Choi, D.; Lemmon, J. P.; Liu, J. Electrochemical Energy Storage for Green Grid. *Chem. Rev.* **2011**, *111*, 3577–3613.
- (4) Ellis, B. L.; Nazar, L. F. Sodium and Sodium-Ion Energy Storage Batteries. *Curr. Opin. Solid State Mater. Sci.* **2012**, *16*, 168–177.
- (5) Kesler, S. E.; Gruber, P. W.; Medina, P. A.; Keoleian, G. A.; Everson, M. P.; Wallington, T. J. Global Lithium Resources: Relative Importance of Pegmatite, Brine and Other Deposits. *Ore Geol. Rev.* **2012**, *48*, 55–69.
- (6) Pan, H.; Hu, Y. S.; Chen, L. Room-Temperature Stationary Sodium-Ion Batteries for Large-Scale Electric Energy Storage. *Energy Environ. Sci.* **2013**, *6*, 2338–2360.
- (7) Palomares, V.; Serras, P.; Villaluenga, I.; Hueso, K. B.; Carretero-González, J.; Rojo, T. Na-Ion Batteries, Recent Advances and Present Challenges to Become Low Cost Energy Storage Systems. *Energy Environ. Sci.* **2012**, *5*, 5884–5901.
- (8) Hong, S. Y.; Kim, Y.; Park, Y.; Choi, A.; Choi, N. S.; Lee, K. T. Charge Carriers in Rechargeable Batteries: Na Ions vs. Li Ions. *Energy Environ. Sci.* **2013**, *6*, 2067–2081.
- (9) Kim, S. W.; Seo, D. H.; Ma, X.; Ceder, G.; Kang, K. Electrode Materials for Rechargeable Sodium-Ion Batteries: Potential Alternatives to Current Lithium-Ion Batteries. *Adv. Energy Mater.* **2012**, *2*, 710–721.
- (10) Slater, M. D.; Kim, D.; Lee, E.; Johnson, C. S. Sodium-Ion Batteries. *Adv. Funct. Mater.* **2013**, *23*, 947–958.
- (11) Palomares, V.; Casas-Cabanas, M.; Castillo-Martínez, E.; Han, M. H.; Rojo, T. Update on Na-based Battery Materials. A Growing Research Path. *Energy Environ. Sci.* **2013**, *6*, 2312–2337.
- (12) Ponrouch, A.; Dedryvère, R.; Monti, D.; Demet, A. E.; Mba, J. M. A.; Croguennec, L.; Masquelier, C.; Johansson, P.; Palacin, M. R. Towards High Energy Density Sodium Ion Batteries Through Electrolyte Optimization. *Energy Environ. Sci.* **2013**, *6*, 2361–2369.
- (13) Pasta, M.; Wessells, C. D.; Huggins, R. A.; Cui, Y. A High-Rate and Long Cycle Life Aqueous Electrolyte Battery for Grid-Scale Energy Storage. *Nat. Commun.* **2012**, *3*, 1149–1155.
- (14) Ponrouch, A.; Marchante, E.; Courty, M.; Tarascon, J. M.; Palacin, M. R. In Search of an Optimized Electrolyte for Na-Ion Batteries. *Energy Environ. Sci.* **2012**, *5*, 8572–8583.
- (15) Nishi, Y. Lithium Ion Secondary Batteries; Past 10 Years and the Future. *J. Power Sources* **2001**, *100*, 101–106.
- (16) Goodenough, J. B.; Kim, Y. Challenges for Rechargeable Li Batteries. *Chem. Mater.* **2010**, *22*, 587–603.

- (17) Sloop, S. E.; Pugh, J. K.; Wang, S.; Kerr, J. B.; Kinoshita, K. Chemical Reactivity of  $\text{PF}_5$  and  $\text{LiPF}_6$  in Ethylene Carbonate/Dimethyl Carbonate Solutions. *Electrochem. Solid-State Lett.* **2001**, *4*, A42–A44.
- (18) Weingärtner, H. Understanding Ionic Liquids at the Molecular Level: Facts, Problems, and Controversies. *Angew. Chem., Int. Ed.* **2008**, *47*, 654–670.
- (19) Armand, M.; Endres, F.; Macfarlane, D. R.; Ohno, H.; Scrosati, B. Ionic-Liquid Materials for the Electrochemical Challenges of the Future. *Nat. Mater.* **2009**, *8*, 621–629.
- (20) Dupont, J.; de Souza, R. F.; Suarez, P. A. Z. Ionic Liquid (Molten Salt) Phase Organometallic Catalysis. *Chem. Rev.* **2002**, *102*, 3667–3692.
- (21) Chen, C. Y.; Matsumoto, K.; Nohira, T.; Hagiwara, R.; Fukunaga, A.; Sakai, S.; Nitta, K.; Inazawa, S. Electrochemical and Structural Investigation of  $\text{NaCrO}_2$  as a Positive Electrode for Sodium Secondary Battery Using Inorganic Ionic Liquid NaFSA–KFSA. *J. Power Sources* **2013**, *237*, 52–57.
- (22) Chen, C. Y.; Matsumoto, K.; Nohira, T.; Hagiwara, R.; Orikasa, Y.; Uchimoto, Y. Pyrophosphate  $\text{Na}_2\text{FeP}_2\text{O}_7$  as a Low-Cost and High-Performance Positive Electrode Material for Sodium Secondary Batteries Utilizing an Inorganic Ionic Liquid. *J. Power Sources* **2014**, *246*, 783–787.
- (23) Yamamoto, T.; Nohira, T.; Hagiwara, R.; Fukunaga, A.; Sakai, S.; Nitta, K.; Inazawa, S. Charge-Discharge Behavior of Tin Negative Electrode for a Sodium Secondary Battery Using Intermediate Temperature Ionic Liquid Sodium Bis(fluorosulfonyl) Amide–Potassium Bis(fluorosulfonyl)amide. *J. Power Sources* **2012**, *217*, 479–484.
- (24) Monti, D.; Jónsson, E.; Palaćin, M. R.; Johansson, P. Ionic Liquid based Electrolytes for Sodium-Ion Batteries:  $\text{Na}^+$  Solvation and Ionic Conductivity. *J. Power Sources* **2014**, *245*, 630–636.
- (25) Noor, S. A. M.; Howlett, P. C.; MacFarlane, D. R.; Forsyth, M. Properties of Sodium-based Ionic Liquid Electrolytes for Sodium Secondary Battery Applications. *Electrochim. Acta* **2013**, *114*, 766–771.
- (26) Yoon, H.; Zhu, H.; Hervault, A.; Armand, M.; MacFarlane, D. R.; Forsyth, M. Physicochemical Properties of *N*-Propyl-*N*-methylpyrrolidinium Bis(fluorosulfonyl)imide for Sodium Metal Battery Applications. *Phys. Chem. Chem. Phys.* **2014**, *16*, 12350–12355.
- (27) Lee, D. H.; Xu, J.; Meng, Y. S. An Advanced Cathode for Na-Ion Batteries with High Rate and Excellent Structural Stability. *Phys. Chem. Chem. Phys.* **2013**, *15*, 3304–3312.
- (28) Tripathi, R.; Wood, S. M.; Islam, M. S.; Nazar, L. F. Na-Ion Mobility in Layered  $\text{Na}_2\text{FePO}_4\text{F}$  and Olivine  $\text{Na}[\text{Fe},\text{Mn}]\text{PO}_4$ . *Energy Environ. Sci.* **2013**, *6*, 2257–2264.
- (29) Zaghbi, K.; Trottier, J.; Hovington, P.; Brochu, F.; Guerfi, A.; Mauger, A.; Julien, C. M. Characterization of Na-based Phosphate as Electrode Materials for Electrochemical Cells. *J. Power Sources* **2011**, *196*, 9612–9617.
- (30) Zhu, Y.; Xu, Y.; Liu, Y.; Luo, C.; Wang, C. Comparison of Electrochemical Performances of Olivine  $\text{NaFePO}_4$  in Sodium-Ion Batteries and Olivine  $\text{LiFePO}_4$  in Lithium-Ion Batteries. *Nanoscale* **2013**, *5*, 780–787.
- (31) Kubota, K.; Tamaki, K.; Nohira, T.; Goto, T.; Hagiwara, R. Electrochemical Properties of Alkali Bis(trifluoromethylsulfonyl)amides and Their Eutectic Mixtures. *Electrochim. Acta* **2010**, *55*, 1113–1119.
- (32) Wongtharom, N.; Lee, T. C.; Wang, C. H.; Wang, Y. C.; Chang, J. K. Electrochemical Performance of Na/ $\text{NaFePO}_4$  Sodium-Ion Batteries with Ionic Liquid Electrolytes. *J. Mater. Chem. A* **2014**, *2*, 5655–5661.
- (33) Fey, G. T. K.; Huang, K. P.; Kao, H. M. A Polyethylene Glycol-Assisted Carbothermal Reduction Method to Synthesize  $\text{LiFePO}_4$  Using Industrial Raw Materials. *J. Power Sources* **2011**, *196*, 2810–2818.
- (34) Bazito, F. F. C.; Kawano, Y.; Torresi, R. M. Synthesis and Characterization of Two Ionic Liquids with Emphasis on Their Chemical Stability Towards Metallic Lithium. *Electrochim. Acta* **2007**, *52*, 6427–6437.
- (35) Oh, S. M.; Myung, S. T.; Hassoun, J.; Scrosati, B.; Sun, Y. K. Reversible  $\text{NaFePO}_4$  Electrode for Sodium Secondary Batteries. *Electrochem. Commun.* **2012**, *22*, 149–152.
- (36) Arbizzani, C.; Gabrielli, G.; Mastragostino, M. Thermal Stability and Flammability of Electrolytes for Lithium-Ion Batteries. *J. Power Sources* **2011**, *196*, 4801–4805.
- (37) Bruce, P. G.; Evans, J.; Vincent, C. A. Conductivity and Transference Number Measurements on Polymer Electrolytes. *Solid State Ionics* **1988**, *28–30*, 918–922.
- (38) Fericola, A.; Croce, F.; Scrosati, B.; Watanabe, T.; Ohno, H. LiTFSI-BEPyTFSI as an Improved Ionic Liquid. *J. Power Sources* **2007**, *174*, 342–348.
- (39) Ramana, C. V.; Mauger, A.; Gendron, F.; Julien, C. M.; Zaghbi, K. Study of the Li-Insertion/Extraction Process in  $\text{LiFePO}_4/\text{FePO}_4$ . *J. Power Sources* **2009**, *187*, 555–564.
- (40) Xia, X.; Lamanna, W. M.; Dahn, J. R. The Reactivity of Charged Electrode Materials with Sodium Bis(trifluoromethanesulfonyl)imide ( $\text{NaTFSI}$ ) based-Electrolyte at Elevated Temperatures. *J. Electrochem. Soc.* **2013**, *160*, A607–A609.
- (41) Lauw, Y.; Horne, M. D.; Rodopoulos, T.; Lockett, V.; Akgun, B.; Hamilton, W. A.; Nelson, R. J. Structure of  $[\text{C}_4\text{mpyr}][\text{NTf}_2]$  Room-Temperature Ionic Liquid at Charged Gold Interfaces. *Langmuir* **2012**, *28*, 7374–7381.
- (42) Andriola, A.; Singh, K.; Lewis, J.; Yu, L. Conductivity, Viscosity, and Dissolution Enthalpy of  $\text{LiNTf}_2$  in Ionic Liquid BMINTF<sub>2</sub>. *J. Phys. Chem. B* **2010**, *114*, 11709–11714.
- (43) Casas-Cabanas, M.; Roddatis, V. V.; Saurel, D.; Kubiak, P.; Carretero-González, J.; Palomares, V.; Serras, P.; Rojo, T. Crystal Chemistry of Na Insertion/Deinsertion in  $\text{FePO}_4$ – $\text{NaFePO}_4$ . *J. Mater. Chem.* **2012**, *22*, 17421–17423.
- (44) Lau, S. C.; Bae, E. G.; Lim, H.; Pyo, M. Non-crystalline Oligopyrene as a Cathode Material with a High-Voltage Plateau for Sodium Ion Batteries. *J. Power Sources* **2014**, *254*, 73–79.
- (45) Komaba, S.; Ishikawa, T.; Yabuuchi, N.; Murata, W.; Ito, A.; Ohsawa, Y. Fluorinated Ethylene Carbonate as Electrolyte Additive for Rechargeable Na Batteries. *ACS Appl. Mater. Interfaces* **2011**, *3*, 4165–4168.